Partial IGF Affinity of Circulating N- and C-Terminal Fragments of Human Insulin-like Growth Factor Binding Protein-4 (IGFBP-4) and the Disulfide Bonding Pattern of the C-Terminal IGFBP-4 Domain†

Ludger Ständker,*,‡ Thomas Braulke,§ Silke Mark,‡ Hossein Mostafavi,‡ Markus Meyer,‡ Stefan Höning,|| Guillermo Giménez-Gallego,⊥ and Wolf-Georg Forssmann‡

The Lower Saxony Institute for Peptide Research (IPF), Feodor-Lynen Strasse 31, D-30625 Hannover, Germany, Children's Hospital, University of Hamburg, D-20246 Hamburg, Germany, Institute for Biochemistry II, University of Göttingen, D-37073 Göttingen, Germany, and Centre de Investigaciones Biológicas, E-28006 Madrid, Spain

Received October 29, 1999; Revised Manuscript Received February 24, 2000

ABSTRACT: Within the IGF axis, the insulin-like growth factor-binding proteins (IGFBPs) are known to play a pivotal role in cell proliferation and differentiation. Defined proteolysis of the IGFBPs is proposed to be an essential mechanism for regulating IGF bioavailability. The generated IGFBP fragments in part exhibit different IGF-dependent and -independent biological activities. Characterizing naturally occurring forms of IGFBPs in human plasma, we identified both a N- and a C-terminal fragment of IGFBP-4 by means of immunoreactivity screening. As a source for peptide isolation, we used large amounts of human hemofiltrate obtained from patients with chronic renal failure. Purification of the IGFBP-4 peptides from hemofiltrate was performed by consecutive cation-exchange and reverse-phase chromatographic steps. Mass spectrometric and sequence analysis revealed an M_r of 13 233 for the purified N-terminal fragment spanning residues Asp^{1}−Phe^{122} of IGFBP-4 and an M_r of 11 344 for the C-terminal fragment extending from Lys^{136} to Glu^{237}. Proteolytic digestion and subsequent biochemical analysis showed that the six cysteines of the C-terminal IGFBP-4 fragment are linked between residues 153−183, 194−205, and 207−228 (disulfide bonding pattern, 1−2, 3−4, and 5−6). Plasmon resonance spectroscopy, ligand blot analysis, and saturation and displacement studies demonstrated a very low affinity of the C-terminal IGFBP-4 fragment for the IGFs (IGF-II, K_d = 690 nM; IGF-I, K_d > 60 nM), whereas the N-terminal fragment retained significant IGF binding properties (IGF-II, K_d = 17 nM; IGF-I, K_d = 5 nM). This study provides the first molecular characterization of circulating human IGFBP-4 fragments formed in vivo exhibiting an at least 5-fold decrease in the affinity of the N-terminal IGFBP-4 fragment for the IGFs and a very low IGF binding capacity of the C-terminal fragment.

The insulin-like growth factor-binding proteins (IGFBPs)[1] are a family of six related proteins involved in regulating the effects and the bioavailability of the insulin-like growth factors, IGF-I and IGF-II, which are responsible for growth and differentiation of cells and tissues (*1*, *2*).

The complete IGFBPs exhibit high affinity for both IGFs and are capable of either enhancing or inhibiting cellular effects of the IGFs. Furthermore, they have partly been shown to exhibit intrinsic activities independent of their binding to the IGFs that modulate cell proliferation (*3*, *4*).

The overall structure of IGFBP-1−6 consists of cysteine-rich, globular N- and C-terminal domains which are connected by a nonconserved central region (*5*). The N-terminal domains include 10−14 cysteine residues, whereas the C-terminal domains of all IGFBPs contain six cysteine residues forming disulfide bonds. It has been reported that either the N-terminal domain of IGFBP-3−5 (*6*−*8*), the C-terminal domain of IGFBP-2 (*9*, *10*), or both domains of IGFBP-3 and -4 (*5*, *7*) bind the IGFs, however, with reduced affinity compared to those of the complete IGFBP molecules.

In human plasma, all six IGFBPs were detectable, mostly occurring as high-molecular mass complexes of 40−50 or 150 kDa, but only little is known about their exact in vivo degradation and the presence of low-molecular mass IGFBP fragments (*2*). Therefore, we started to screen for circulating fragments of IGFBPs in human blood filtrate (hemofiltrate, HF) (*11*, *12*) to identify the cleavage sites formed in vivo and to characterize structural and functional properties of the fragments themselves.

Human HF is generated during blood filtration of patients with endstage renal disease and was hitherto shown to be a valuable source for the isolation of new regulatory peptides with M_rs of <20000 (*13*, *14*).

This study provides the first structural description of circulating human IGFBP-4 fragments formed in vivo. We purified both a 13.2 kDa N-terminal fragment of IGFBP-4 bearing significant IGF affinity and an 11.3 kDa C-terminal fragment with only very low IGF binding capacity. The

† Supported by the German government, BMBF Grant 0311139, and the Deutsche Forschungsgemeinschaft (SFB 402/A6; T.B.).

* To whom correspondence should be addressed. Phone: +49-(0)-511-5466-329. Fax: +49-(0)511-5466-132. E-mail: L.standker@gmx.net.

‡ The Lower Saxony Institute for Peptide Research.

§ University of Hamburg.

|| University of Göttingen.

⊥ Centre de Investigaciones Biológicas.

[1] Abbreviations: ESI-MS, electrospray ionization mass spectrometry; HF, hemofiltrate; MALDI-MS, matrix-assisted laser desorption ionization mass spectrometry; IGF, insulin-like growth factor; IGFBP, insulin-like growth factor binding protein; rh, recombinant human; SDS−PAGE, sodium dodecyl sulfate−polyacrylamide gel electrophoresis.

10.1021/bi992513s CCC: $19.00
Published on Web 04/07/2000

disulfide bonding pattern of the C-terminal fragment was determined (connected cysteines, 1−2, 3−4, and 5−6). Our data indicate a high level of structural stability of both IGFBP domains in the circulation.

MATERIALS AND METHODS

Isolation of N- and C-Terminal IGFBP-4 Fragments. The peptide bank used as a source for the isolation of IGFBP-4 peptides was generated from 10 000 L of human blood ultrafiltrate (hemofiltrate, HF) as described recently (*13*). In brief, peptides were extracted by cation-exchange chromatography using seven buffers with increasing pH followed by RP chromatography of the resulting pH eluates. Lyophilized aliquots of the peptide bank fractions corresponding to 100 mL equivalents of human hemofiltrate were used to detect IGFBP-4 peptides by Western blot analysis. Isolation of both intensive immunoreactivities with apparent molecular masses in the range of 11−14 kDa corresponding to the C- and N-terminal IGFBP-4 fragments, respectively, was performed by consecutive chromatographic steps. The C-terminal fragment was purified by two additional RP chromatographic separations. As solvents in gradient elution, 0.1% TFA in H_2O (solvent A) and 80% (v/v) acetonitrile containing 0.1% TFA (solvent B) were used. First, the fraction exhibiting the 11 kDa immunoreactivity was applied to an analytical RP-C4 column (250 mm × 20 mm inside diameter, 30 nm, 5 μm, Vydac, Hesparia, CA) at a flow rate of 2.5 mL/min with a linear gradient from 100% solvent A to 80% solvent B over the course of 80 min. Final purification was performed using an analytical RP-C18 column (250 mm × 4.6 mm inside diameter, 30 nm, 5 μm, Vydac) at a flow rate of 0.7 mL/min (linear gradient from 100% solvent A to 60% solvent B over the course of 60 min). Isolation of the N-terminal IGFBP-4 fragment was carried out as described recently (*12*).

SDS−PAGE and Western Immunoblotting. Lyophilized aliquots of HPLC fractions corresponding to 100 mL equivalents of hemofiltrate were reconstituted in sample buffer, and the peptides were separated by SDS−PAGE (*15*) in Mini-Protean systems (Bio-Rad, Munich, Germany) for 20 min at 60 V followed by 100 min at 120 V. Molecular mass standards of 4−210 kDa (SeeBlue, NOVEX, San Diego, CA) were used as references. The separated peptides were transferred to a hydrophilic poly(vinylidene difluoride) (PVDF) membrane at 7 V for 2 h using a semidry electrophoretic transfer unit (Bio-Rad). After incubation with rabbit anti-IGFBP-4 antiserum (Upstate Biotechnology, Lake Placid, NY) diluted to 1:1000, the membrane was incubated with anti-rabbit IgG coupled to alkaline phosphatase (Sigma, Deisenhofen, Germany). Bands were developed using a bromochloroindolyl phosphate/nitro blue tetrazolium substrate systems as recommended by the manufacturer (Sigma). Immunoreactive fractions were additionally analyzed by mass spectrometry.

Peptide Analysis. Mass determination of the purified peptides was carried out on a Sciex API *III* quadrupole mass spectrometer (Sciex, Perkin-Elmer, Langen, Germany) with an electrospray interface (ESI-MS). Mass analysis of HPLC fractions was performed with a LaserTec RBT II MALDI-MS system (PerSeptive Biosystems, Freiburg, Germany) as described previously (*12*).

Peptides were sequenced on a 473 A gas-phase sequencer (Applied Biosystems, Weiterstadt, Germany) by Edman degradation with on-line detection of phenylthiohydantoin amino acids using the standard protocol recommended by the manufacturer.

Identification of the C-terminal amino acids of IGFBP-4^{1-122} was carried out as described in detail previously (*16*). Briefly, 50 μg of the peptide was immobilized to a poly(vinylidene difluoride) matrix, which was digested with carboxypeptidase P (sequencing grade from Boehringer Mannheim, Mannheim, Germany) at 37 °C in 50 mM sodium citrate (pH 4.0). After digestion for 0.5, 1, 3, 5, and 10 min, cleaved C-terminal amino acids were identified by conventional amino acid analysis.

To analyze the disulfide bonding pattern of IGFBP-$4^{136-237}$, proteolytic cleavage of the native peptide was performed by the endoproteases chymotrypsin and Arg-C (sequencing grade from Boehringer Mannheim). For chymotryptic digestion, the peptide was incubated using a peptide:enzyme ratio of 100:1 (w/w) for 8 h at 25 °C in Tris-HCl buffer (pH 7.8, 100 mM) as recommended by the manufacturer. For Arg-C digestion, incubation was performed using a peptide:enzyme ratio of 100:1 (w/w) for 2 h at 37 °C in Tris-HCl buffer (pH 7.6, 90 mM) according to the manufacturer's instructions. The resulting fragments were separated by analytical RP-C18 HPLC and analyzed by mass spectrometry (MALDI-MS) first. Peaks containing masses corresponding to calculated masses of expected fragments containing disulfide bonds were sequenced and analyzed by ESI-MS.

Surface Plasmon Resonance Interaction Analysis, IGF Competition Studies, and Ligand Blotting. IGFs were purchased from PeproTech (London, U.K.). Intact recombinant human IGFBP-4 (rhIGFBP-4) was kindly provided by K. Lang (Penzberg, Germany).

The interaction between intact IGFBP-4 or IGFBP-4 fragments and IGF-II was analyzed in real time by surface plasmon resonance using a BIAcore-2000 biosensor (Pharmacia, Freiburg, Germany). IGF-II was coupled to a CM5 sensor chip via amino coupling (2 ng/mm^2). All interaction experiments were performed in buffer A [20 mM HEPES/NaOH (pH 7.0), 150 mM NaCl, 10 mM KCl, and 2 mM $MgCl_2$] at a flow rate of 20 μL/min. Association for 2 min was followed by dissociation for 2 min, during which buffer A was perfused. A short pulse injection (15 s) of 20 mM NaOH/0.5% SDS was used to regenerate the sensor chip surface after each experimental cycle. The peptide-derivatized sensor chips remained stable and retained their specific binding capacity for more than 100 experimental cycles of association/dissociation and regeneration. The rate constants (k_a for association and k_d for dissociation) of the interactions were calculated with the BIAevaluation software, version 1.2. [^{125}I]IGF-II ligand blotting was performed as described previously (*17*).

Furthermore, saturation and displacement studies using radiolabeled and unlabeled IGF-I and -II were performed. First, increasing concentrations of each binding protein were incubated with 20 000 cpm of [^{125}I]IGF-I or -II (specific activity of ca. 500 000 cpm/ng) for 22−24 h at 4 °C in a total volume of 300 μL of assay buffer [0.1 M HEPES, 0.44 mM $NaHCO_3$, 0.02% Triton X-100, and 0.1% BSA (pH 6.0)]. Bound and free IGF were separated by adding 500 μL of 40% (w/v) polyethylene glycol 4000 in assay buffer. The samples were mixed vigorously, incubated for 30 min at room temperature, and centrifuged at 2000*g* for 25 min at 4 °C. The supernatant was removed, and the samples were

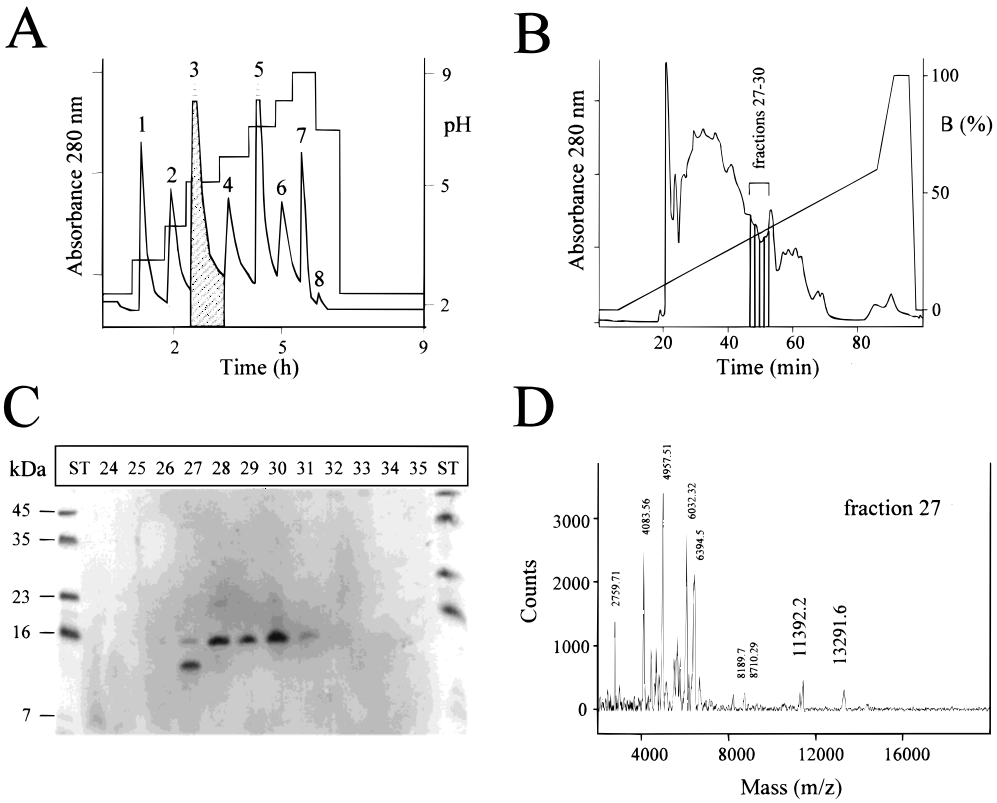

FIGURE 1: Detection of immunoreactive IGFBP-4 fragments in human hemofiltrate. Isolation of the immunoreactive IGFBP-4 fragments was guided by immunoblot screening in fractions of a peptide bank established from human hemofiltrate comprising about 350 different peptide-containing fractions. (A) In a first separation step using cation-exchange chromatography, peptides were batchwise eluted by means of a pH gradient. (B) RP-HPLC fractionation of the peptides derived from pH pool eluate 3. (C) Aliquots of this chromatography were examined by immunoblotting using polyclonal anti-IGFBP-4 antibodies. Two main immunoreactive peptides with apparent masses of 12 and 14 kDa could be detected in fractions 27−30. (D) The MALDI-MS spectrum of fraction 27 from pH pool eluate 3 containing both immunoreactive IGFBP-4 peptides exhibited molecular masses of 11.4 and 13.3 kDa.

centrifuged again at 2000*g* for 20 min. The bound radioactivity in the final pellet was measured by γ-counting (1470 Wallac Wizard, Pharmacia, Turku, Finland). Nonspecific binding was quantitated by adding a 500-fold excess of unlabeled IGF and subtracted from the total bound radioactivity to determine the extent of specific binding. The IGFBP concentrations yielding 40−50% binding of radiolabeled IGFs were used to construct displacement curves in the presence of increasing concentrations of unlabeled IGF-I or -II using the same protocol as described above. K_d values were determined by nonlinear curve fitting and Scatchard analysis.

RESULTS

Detection of Immunoreactive IGFBP-4 Peptides in Hemofiltrate and Purification of N- and C-Terminal IGFBP-4 Fragments. Human hemofiltrate was previously described as a valuable source for the isolation of regulatory peptides with M_rs of <20000 (*13*, *14*). To identify circulating fragments of the insulin-like growth factor binding proteins (IGFBPs), we performed immunoblotting in the fractions of a peptide bank generated from 10 000 L of hemofiltrate as described recently (*11*, *12*).

Generation of the peptide bank fractions was achieved in a standardized two-step procedure, including stepwise batch elution from a cation exchanger with seven buffers with increasing pH (Figure 1A) and subsequent fractionation of the resulting pH pool eluates by RP chromatography (Figure 1B). Aliquots of these fractions were examined using polyclonal anti-IGFBP-4 antibodies. The fractions obtained after reverse-phase chromatography of pH pool eluate 3 revealed the existence of two prominent IGFBP-4 immunoreactive bands exhibiting apparent molecular masses of 12 and 14 kDa (Figure 1C). MALDI-MS analysis of fraction 27 containing both immunoreactive bands revealed peptides with molecular masses of 11.4 and 13.3 kDa (Figure 1D).

The immunoreactive peptide with an apparent molecular mass of 14 kDa was subsequently purified from fraction 29 of pH pool eluate 3 using additional chromatographic steps (*12*), accompanied by immunoblotting and MALDI-MS as depicted in panels C and D of Figure 1. Finally, analytical reverse-phase chromatography (Figure 2A) resulted in a pure peptide as demonstrated by capillary zone electrophoresis (inset in Figure 2A). The exact molecular mass of the peptide determined by ESI-MS was 13 233 ± 1.1 Da (Figure 2B). N-Terminal sequence analysis yielded the sequence DEAIHXPPXSEEKLARXRPP (where X represents a weak amino acid signal that could not be assigned), indicating the isolation of an N-terminal fragment of human IGFBP-4 (Figure 2C). The determined molecular mass of 13 233 Da was in accordance with the calculated mass of IGFBP-4^{1-122} (13 237 Da). After reduction and amidoalkylation of the N-terminal IGFBP-4 fragment, the molecular mass was determined to be 14 042 ± 2.9 Da, indicating 14 alkylated cysteine residues (mass increase of 58 Da for each cysteine). C-Terminal sequence analysis following carboxypeptidase

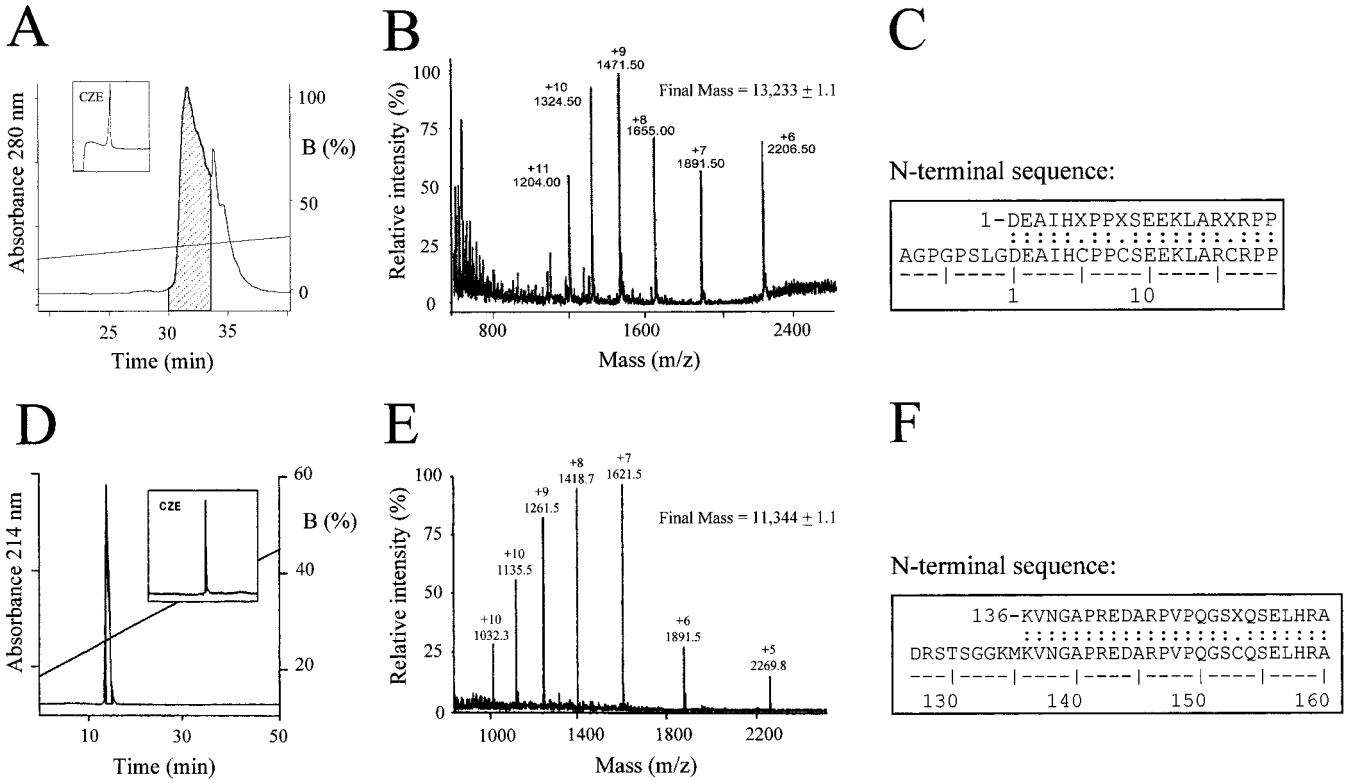

FIGURE 2: Purification and analysis of the immunoreactive N- and C-terminal IGFBP-4 fragments. (A) Purification of the 13.3 kDa immunoreactive peptide from fraction 29 (panels B and C of Figure 1) was achieved by consecutive chromatographic steps (not shown) and yielded in isolation a pure peptide by final analytical RP-HPLC. The purity of the peptide was checked by capillary zone electrophoresis (CZE; inset). (B) The ESI-MS spectrum exhibited a molecular mass of 13 233 ± 1.1 Da. (C) N-Terminal sequence analysis of the purified immunoreactive peptide and alignment with the human IGFBP-4 sequence revealed isolation of an N-terminal IGFBP-4 peptide. (D) Further chromatographic purification of immunoreactive fraction 27 (panels B and C of Figure 1) was performed (not shown), and final reverse-phase chromatography yielded in isolation of a pure peptide as demonstrated by capillary zone electrophoresis (CZE; inset). (E) The molecular mass was determined to be 11 344 ± 1.1 Da by ESI-MS. (F) N-Terminal sequence analysis and alignment with the human IGFBP-4 sequence showed isolation of a C-terminal IGFBP-4 fragment starting with Lys^{136}.

P digestion revealed that the sequence QKHF constitutes the four C-terminal amino acid residues of the peptide (119−122). Taken together, all data are consistent with the isolation of an N-terminal IGFBP-4 fragment from human hemofiltrate comprising the 1−122.

Using the same procedure, the immunoreactive band of approximately 12 kDa in fraction 27 of pH pool eluate 3 (Figure 1C) was isolated by consecutive chromatographic steps. The final reverse-phase chromatography (Figure 2D) yielded a pure peptide as shown by capillary zone electrophoresis (inset in Figure 2D). The peptide exhibited a molecular mass of 11 344 ± 1.1 Da that was determined by ESI-MS (Figure 2E). Initially, 25 amino acid residues of the N-terminus were sequenced, which demonstrated the isolation of a C-terminal fragment of human IGFBP-4 starting with Lys^{136} (Figure 2F). The determined molecular mass was in accordance with the theoretical mass of residues 136−237 of human IGFBP-4, calculated to be 11 347 Da. These results indicate that Glu^{237} is the C-terminal amino acid residue of the C-terminal IGFBP-4 fragment isolated from hemofiltrate.

Disulfide Bonding of the IGFBP-4$^{136-237}$ Fragment. Milligram amounts of the N- and C-terminal IGFBP-4 fragment were isolated from 10 000 L of human hemofiltrate and purified to homogeneity. For determination of the disulfide bonding pattern of C-terminal IGFBP-4$^{136-237}$, proteolytic digestion of the peptide with subsequent MALDI-MS, ESI-MS, and sequence analysis was carried out. The molecular

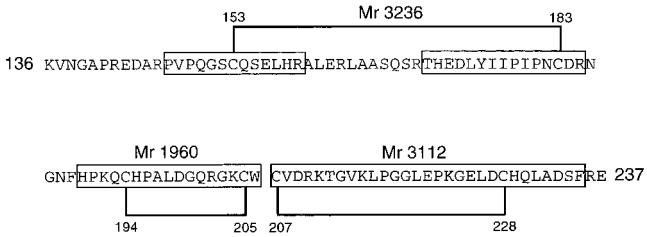

FIGURE 3: Disulfide bonding pattern of the human IGFBP-4 C-terminal domain. The native peptide IGFBP-4$^{136-237}$ was cleaved by endoproteases Arg-C and chymotrypsin as described in Materials and Methods. The resulting fragments analyzed by MALDI-MS, ESI-MS, and sequencing are represented by gray boxes. Two connected fragments of the endoprotease Arg-C digest (molecular mass of 3236 Da) were shown to comprise amino acid residues 147−159 and 171−185 and indicated the existence of a disulfide bond between Cys^{153} and Cys^{183}. Two single fragments derived from chymotryptic digestion of IGFBP-4$^{136-237}$ with molecular masses of 1960 and 3112 Da belonged to amino acid residues 190−206 and 207−235, respectively, indicating disulfide bridges between Cys^{194} and Cys^{205} and Cys^{207} and Cys^{228} in the native IGFBP-4 fragment.

mass of the reduced and amidoalkylated IGFBP-4$^{136-237}$ fragment was determined to be 11 692 ± 1.5 Da, indicating six amidoalkylated cysteine residues (mass increase of 58 Da for each cysteine). The native IGFBP-4$^{136-237}$ fragment was cleaved by the endoproteases Arg-C and chymotrypsin (Figure 3). Sequencing of a 3236 Da fragment obtained from Arg-C digestion yielded two amino acid signals per cycle which could be assigned to amino acid residues 147−159

and 171−185 by computer analysis. These results demonstrate the existence of a disulfide bond between Cys^{153} and Cys^{183}. Another fragment with a molecular mass of 1960 Da derived from chymotryptic digest of IGFBP-$4^{136-237}$ represented residues 190−206, and a further fragment with a molecular mass of 3112 Da comprised amino acid residues 207−235 (Figure 3). These data are compatible with disulfide linkages between Cys^{194} and Cys^{205} and Cys^{207} and Cys^{228}, respectively. In summary, the isolated human C-terminal IGFBP-4 fragment contains three disulfide linkages between cysteines 153 and 183, 194 and 205, and 207 and 228 (bonding pattern, 1−2, 3−4, and 5−6).

IGF Binding Properties of the Isolated N- and C-Terminal Fragments of IGFBP-4. To examine the ability of the isolated N- and C-terminal IGFBP-4 fragments to bind to the IGFs, the fragments were separated by SDS−PAGE and blotted onto nitrocellulose membranes followed by incubation with either [^{125}I]IGF-II (Figure 4A) or anti-IGFBP-4 antibody (Figure 4B). While 50 ng of intact recombinant human IGFBP-4 and 250 ng of IGFBP-$4^{136-237}$ bound similar amounts of [^{125}I]IGF-II (determined by densitometry and direct counting of the excised bands from the nitrocellulose membrane), no binding of [^{125}I]IGF-II to 250 ng of the IGFBP-$4^{136-237}$ fragment was observed (Figure 4A). For comparison, aliquots of hemofiltrate fractions containing both peptides (comparable to fraction 27 as shown in panels C and D of Figure 1) were pooled and subsequently tested by immunoblotting and ligand blotting. After immunoblotting had been performed, the pooled fraction contained the major 14 and 12 kDa IGFBP-4 fragments mentioned above, and minor IGFBP-4 immunoreactive bands of 21 and 18 kDa (Figure 4B). When tested in ligand blotting, the 14 kDa but not the 12 kDa fragment bound [^{125}I]IGF-II, confirming the data obtained with the purified N- and C-terminal fragments (Figure 4A). Furthermore, only the minor IGFBP-4 immunoreactive band of 18 kDa bound [^{125}I]IGF-II (Figure 4A). This 18 kDa band was analyzed by direct sequencing, yielding the N-terminus of IGFBP-4. By [^{125}I]IGF-II ligand blotting, traces of intact IGFBP-4 were also detected in the pooled fraction which could not be seen by IGFBP-4 immunoblotting.

In a second approach, the precise rate constants (k_a, k_d, and K_d) for the interaction between the IGFBP-4 fragments, intact rhIGFBP-4, and IGF-II were determined by surface plasmon resonance spectroscopy. IGF-II was immobilized on a sensor surface, and subsequently, recombinant human IGFBP-4 or one of the purified fragments was passed over the IGF-derivatized surface and analyzed for binding (Figure 4C). A high-affinity binding of intact rhIGFBP-4 (K_d = 1.7 nM) to IGF-II was identified, the rate of which was 10-fold reduced using IGFBP-4^{1-122} (K_d = 17 nM). The affinity, however, of the C-terminal IGFBP-$4^{136-237}$ fragment was estimated to be more than 400-fold lower for IGF-II (K_d = 690 nM) than for the intact IGFBP-4. Thus, although the affinity of intact IGFBP-4 for IGF-II is underestimated in the biosensor experiments, the results demonstrate the significantly lower affinity of both but especially of the C-terminal IGFBP-$4^{136-237}$ fragment for IGF-II. These results were confirmed by saturation and displacement studies using radiolabeled and unlabeled IGF-II (data not shown). Affinity constants for the binding to IGF-I were also determined by saturation and displacement experiments (Figure 4D). Whereas the N-terminal IGFBP-4^{1-122} fragment exhibited a 5-fold reduced IGF-I binding affinity (K_d = 5 nM) compared to that of the complete IGFBP-4 (K_d = 1.2 nM), the C-terminal IGFBP-$4^{136-237}$ fragment revealed an even more reduced IGF-I binding affinity (K_d > 60 nM). Comparable values were obtained by sedimentation equilibrium measurements by centrifuging an equimolar mixture of each fragment together with IGF-I (data not shown).

DISCUSSION

This study provides the first purification and biochemical characterization of circulating human IGFBP-4 fragments formed in vivo. The results demonstrate that both the N-terminal (IGFBP-4^{1-122}) and C-terminal (IGFBP-$4^{136-237}$) fragments are present in the circulation and bind IGF-I and -II, although with reduced affinity.

The formation of IGFBP fragments by limited proteolysis of their parent IGFBP molecules results in a reduced affinity for the IGFs and decreases the half-life of the circulating growth factors (*18*−*20*) which makes the IGFs more available for interaction with cellular IGF receptors. Our findings confirm this concept, demonstrating an at least 5-fold decrease in the affinity of the IGFBP-4^{1-122} fragment for both IGF-I and IGF-II and a further reduction of IGF binding capacity of the C-terminal fragment. Recently, mutational analysis of human IGFBP-4 revealed that residues 72−91 located in the N-terminal region are essential for IGF binding (*7*). Although the main IGF binding site in various IGFBPs appears to be located in the N-terminal part (*8*, *21*), the C-terminal domain is also shown to retain IGF binding capacity (*10*, *22*). It is suggested that both domains contribute to the high-affinity binding of the intact IGFBP (*5*, *22*).

Proteolytic activities cleaving IGFBP-4 into 18 and 14 kDa fragments have been identified in media of various cultured cells (*23*). Interestingly, the 18 kDa immunoreactive band detected in pooled hemofiltrate fractions (Figure 4B) exhibited the N-terminal sequence of IGFBP-4 and might therefore be a glycosylated form of the IGFBP-4^{1-122} fragment, since the potential N-glycosylation site (Asn^{101}) is located in the N-terminal sequence. This N-terminal 18 kDa IGFBP-4 fragment also exhibited significant IGF-II binding properties (Figure 4A).

In human serum, proteolysis of IGFBP-4 has been observed transiently after bypass surgery (*24*) and in pregnancy catalyzed by a disintegrin metalloprotease (*25*). Because the proteolytic cleavage sites of human IGFBP-4 used by this serum protease are unknown, the potential identity with the protease(s) generating IGFBP-4^{1-122} and IGFBP-$4^{136-237}$ fragments remains to be determined. On the other hand, whereas fragmented forms of IGFBP-2, -3, and -5 are also found in the hemofiltrate of patients suffering from chronic renal disease (*11*, *21*; L. Ständker, unpublished results), almost nothing is known about IGFBP fragments in the circulation of healthy, nonpregnant individuals. Therefore, it is unclear whether the amounts of IGFBP-4 fragments isolated from hemofiltrate represent elevated levels as reported for a 29 kDa IGFBP-3 fragment (*21*) since comparable serum samples from healthy probands are not available. The serum of patients with renal disease for IGFBP-4 protease activity in vitro resembles that of nonpregnancy rather than pregnancy serum (T. Braulke, unpublished observations). This indicates that the nanomolar

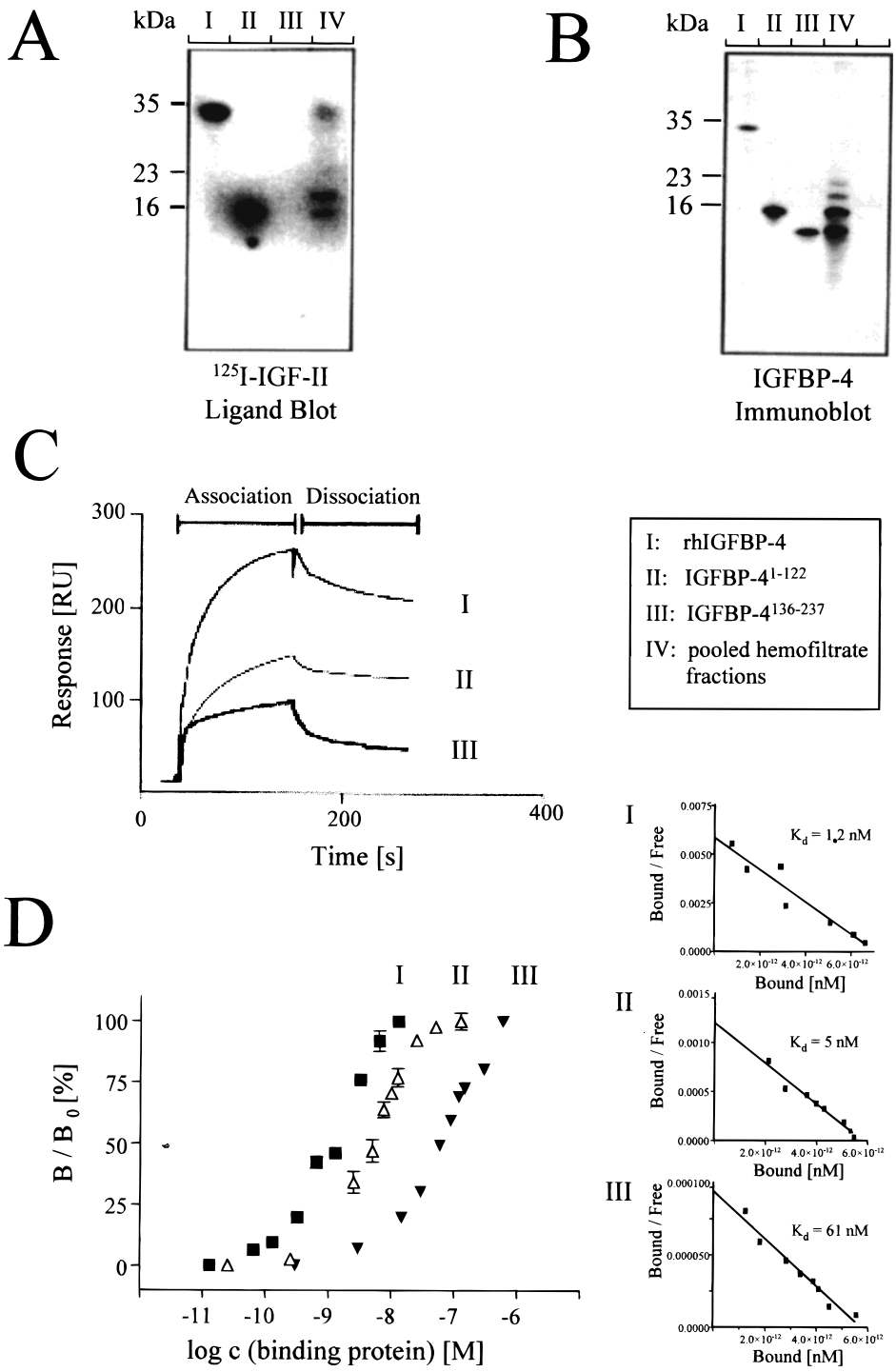

FIGURE 4: Binding of IGF-I and IGF-II to intact IGFBP-4 and its circulating fragments. Intact rhIGFBP-4 (50 ng), purified N-terminal IGFBP-4$^{1-122}$ and C-terminal IGFBP-4$^{136-237}$ fragments (250 ng each), and a pooled hemofiltrate fraction containing both immunoreactive IGFBP-4 fragments (as shown in panels C and D of Figure 1) were separated by SDS−PAGE and analyzed in parallel by (A) [^{125}I]IGF-II ligand blotting and (B) IGFBP-4 immunoblotting. Note also traces of intact IGFBP-4 and a 18 kDa fragment of IGFBP-4 in the pooled hemofiltrate fraction in ligand blot analysis (A) and minor immunoreactive bands of 18 and 21 kDa (B). The positions of the molecular mass markers are indicated. The data shown in panels A and B are from a representative experiment out of three. (C) Biacore experiments showed high-affinity binding of intact rhIGFBP-4 to immobilized IGF-II (K_d = 1.7 nM), whereas IGFBP-4$^{1-122}$ and IGFBP-4$^{136-237}$ exhibited 10- and 400-fold reduced IGF-II binding affinity, respectively. The curves that are shown represent the sum of at least six binding cycles. (D) Saturation binding studies and Scatchard analysis of complete rhIGFBP-4 and the purified N-terminal IGFBP-4$^{1-122}$ and C-terminal IGFBP-4$^{136-237}$ fragments using [^{125}I]IGF-I confirmed the reduced affinity of binding of IGFBP-4$^{1-122}$ and a very low affinity of binding of IGFBP-4$^{136-237}$ to IGF-I. The binding data represent the summary of two different experiments performed in triplicate. The bars indicate the standard error of the mean.

concentrations of the purified IGFBP-4 fragments might not be due to an increased level of serum proteolysis. Reduced clearance of peptides by insufficient kidney function as suggested for IGFBP-3 fragments (*26*) or the generation of fragments in nonvascular compartments cannot be excluded. It is likely that at least two proteases are involved in IGFBP-4 proteolysis in the central, nonconserved region cleaving between residues Phe^{122} and Ala^{123} and between Met^{135} and

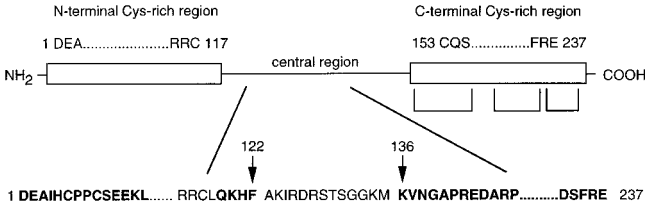

FIGURE 5: Schematic diagram of the IGFBP-4 structure and proteolytic cleavage sites as detected in human hemofiltrate. The cysteine-rich highly conserved regions of IGFBP-4 are represented as shaded boxes. Sequenced amino acids are in bold letters. In vivo proteolytic cleavage sites in the central nonconserved region are marked by arrows resulting in generation of circulating N-terminal 13.2 kDa (IGFBP-4^{1-122}) and the C-terminal 11.3 kDa (IGFBP-$4^{136-237}$) fragments. The disulfide bonds of the C-terminal region are indicated below the diagram.

Lys^{136} (Figure 5). Possibly, chymotrypsin-like proteases catalyze the cleavage between Phe^{122} and Ala^{123}. Tissue kallikreins known to hydrolyze peptide bonds between methionine and lysine residues in circulating kininogen (*27*) may be responsible for the generation of the C-terminal IGFBP-4 fragment starting with Lys^{136}. Fragments also starting with Lys^{136} derived from human IGFBP-4 or with the homologous Lys^{132} from rat IGFBP-4 are generated by a protease secreted by human fibroblasts (*23*) or by a glucocorticoid-inducible protease in media from rat B104 cells (*28*), respectively, which appear to be metalloserine proteases according to their inhibitor profiles. Indeed, the IGF-dependent IGFBP-4 protease in human fibroblast-conditioned media was recently identified as the Zn^{2+}-containing pregnancy-associated plasma protein-A (*29*). This protease, however, is different from the IGF-independent IGFBP-4 protease in pregnancy serum (*25*; B. Kübler and T. Braulke, unpublished results). In addition, it is also possible that acidic proteases such as cathepsin D which have been shown to cleave human IGFBP-4 at Met^{135} (*30*) or carboxy- and aminopeptidases are involved in a sequential manner in generating the circulating IGFBP-4^{1-122} and IGFBP-$4^{136-237}$ fragments (Figure 5).

The data from the study presented here show that the conserved N- and C-terminal domains are not linked by disulfide bonds. In addition, the disulfide linkages between Cys^{153} and Cys^{183}, Cys^{194} and Cys^{205}, and Cys^{207} and Cys^{228} involve all cysteine residues in the C-terminal IGFBP-4 domain (Figures 3 and 5). Our results confirm the recent report on the C-terminal disulfide bonding pattern of bovine IGFBP-2 (*10*) in which a similar C-terminal domain structure in every IGFBP has been proposed (pattern, 1−2, 3−4, and 5−6). Since the N-terminal IGFBP-4 domain contains 14 cysteine residues, we were not able to determine this complex disulfide bonding pattern. Future studies will focus on IGF-dependent and -independent biological activities of the circulating N- and C-terminal IGFBP fragments.

ACKNOWLEDGMENT

We thank Ute Block for excellent technical assistance and Bernd Kübler and Rosa M. Lozano for helpful discussions and experimental support.

REFERENCES

1. Shimasaki, S., and Ling, N. (1991) *Prog. Growth Factor Res. 3*, 243−266.
2. Zapf, J. (1995) *Eur. J. Endocrinol. 132*, 645−654.
3. Oh, Y., Müller, H. L., Pham, H., and Rosenfeld, R. G. (1993) *J. Biol. Chem. 268*, 26045−26048.
4. Lalou, C., Lassarre, C., and Binoux, M. (1996) *Endocrinology 137*, 3206−3212.
5. Spencer, E. M., and Chan, K. (1995) *Prog. Growth Factor Res. 6*, 209−214.
6. Vorwerk, P., Yamanaka, Y., Spagnoli, A., Oh, Y., and Rosenfeld, R. G. (1998) *J. Clin. Endocrinol. Metab. 83*, 1392−1395.
7. Qin, X., Strong, D. D., Baylink, D. J., and Mohan, S. (1998) *J. Biol. Chem. 273*, 23509−23516.
8. Kalus, W., Zweckstetter, M., Renner, C., Sanchez, Y., Georgescu, J., Grol, M., Demuth, D., Schumacher, R., Lang, K., and Holak, T. A. (1998) *EMBO J. 17*, 6558−6572.
9. Hobba, G. D., Lothgren, A., Holmberg, E., Forbes, B. E., Francis, G. L., and Wallace, J. C. (1998) *J. Biol. Chem. 273*, 19691−19698.
10. Forbes, B. E., Turner, D., Hodge, S. J., McNeil, K. A., Forsberg, G., and Wallace, J. C. (1998) *J. Biol. Chem. 273*, 4647−4652.
11. Ständker, L., Wobst, P., Mark, S., and Forssmann, W. G. (1998) *FEBS Lett. 441*, 281−286.
12. Mark, S., Forssmann, W. G., and Ständker, L. (1999) *J. Chromatogr., A 852*, 197−205.
13. Schulz-Knappe, P., Schrader, M., Ständker, L., Richter, R., Hess, R., Jürgens, M., and Forssmann, W. G. (1997) *J. Chromatogr. 776*, 125−132.
14. Richter, R., Schulz-Knappe, P., Schrader, M., Ständker, L., Jürgens, M., Tammen, H., and Forssmann, W. G. (1999) *J. Chromatogr., B 726*, 25−35.
15. Schägger, H., and von Jagow, G. (1987) *Anal. Biochem. 166*, 368−379.
16. Sillard, R., Schulz-Knappe, P., Vogel, P., Raida, M., Bensch, K. W., Forssmann, W. G., and Mutt, V. (1993) *Eur. J. Biochem. 216*, 429−436.
17. Hossenlopp, P., Seurin, D., Segovia-Quinson, B., Hardouin, S., and Binoux, M. (1986) *Anal. Biochem. 154*, 138−143.
18. Davenport, M. L., Clemmons, D. R., Miles, M. V., Camacho-Hubner, C., D'Ercole, A. J., and Underwood, L. E. (1990) *Endocrinology 127*, 1278−1286.
19. Holly, J. M., Claffey, D. C., Cwyfan-Hughes, S. C., Frost, V. J., and Yateman, M. E. (1993) *Growth Regul. 3*, 88−91.
20. Blat, C., Villandy, J., and Binoux, M. (1994) *J. Clin. Invest. 93*, 2286−2290.
21. Durham, S. K., Mohan, S., Liu, F., Baker, B. K., Lee, P. D., Hintz, R. L., Conover, C. A., and Powell, D. R. (1997) *Pediatr. Res. 42*, 335−341.
22. Ho, J., and Baxter, R. C. (1997) *Endocrinology 138*, 3811−3818.
23. Conover, C. A., Durham, S. K., Masiarz, F. R., and Kiefer, M. C. (1995) *J. Biol. Chem. 270*, 4395−4400.
24. Cwyfan-Hughes, S. C., Cotterill, A. M., Molloy, A. R., Cassell, T. B., Braude, N., Hinds, C. J., Wass, J. A. H., and Holly, J. M. P. (1992) *J. Endocrinol. 135*, 135−145.
25. Kübler, B., Cowell, S., Zapf, J., and Braulke, T. (1998) *Endocrinology 139*, 1556−1563.
26. Powell, D. R., Liu, F., Baker, B., Lee, P. D. K., Belsha, C. W., Brewer, E. D., and Hintz, R. L. (1993) *Pediatr. Res. 33*, 136−143.
27. Clements, J. A., et al. (1989) *Endocr. Rev. 10*, 393−419.
28. Chernausek, S. D., Smith, C. E., Duffin, K. L., Busby, W. H., Wright, G., and Clemmons, D. R. (1995) *J. Biol. Chem. 270*, 11377−11882.
29. Lawrence, J. B., Oxvig, C., Overgaard, M. T., Sottrup-Jensen, L., Gleich, G. J., Hays, L. G., Yares, J. R., III, and Conover, C. A. (1999) *Proc. Natl. Acad. Sci. U.S.A. 96*, 3149−3153.
30. Claussen, M., Kübler, B., Wendland, M., Neifer, K., Schmidt, B., Zapf, J., and Braulke, T. (1997) *Endocrinology 138*, 3797−3803.

BI992513S